

Transforming low-quality sand into construction materials under 110°C and Recycling of the Waste Solution

Pengcheng Qiu^{1*} and Yuya Sakai¹

¹Institute of Industrial Science, The University of Tokyo, 4-6-1 Komaba, Meguro, Tokyo 153-8505, Japan, qpctju@hotmail.com (Corresponding Author), ysakai@iis.u-tokyo.ac.jp

Abstract. *A strong and eco-friendly material was transformed from low-quality sand via sol-gel method with ethanol as the solvent. 110°C was chosen as a target temperature because it is the average day temperature of the moon, which may be the first place for extraterrestrial development. The appropriate KOH content and ethanol concentration can improve the reaction degree and limit the side reaction. The main results indicated that the highest compressive strength (38 MPa) of the produced material could be obtained by using 20 mass% KOH and 90 V/V% ethanol. According to XRD and FTIR analysis, the formation of sanidine, zeolite, and tetraethoxysilane is the main reason for strength enhancement. Sanidine and zeolite could fill the gap between sand particles and tetraethoxysilane is a good consolidate. Excess ethanol in the waste solution can be reused with recycle rate above 65%. The total carbon emission is 197 kg CO₂ eq/m² after recycling waste solution, which is 35.82% of that produced by normal concrete. Therefore, a tough construction material can be synthesized from low-quality sand, which can partially substitute concrete. This material can address the shortage of raw materials for concrete and can be utilised for extra-terrestrial construction.*

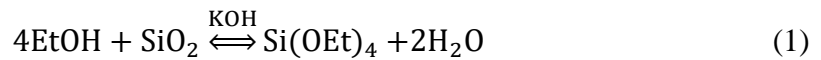
Keywords: *Low-quality sand; Low reaction temperature; extra-terrestrial construction; Recycling; Life-cycle assessment*

1 Introduction

With increasing urbanisation, the demand for sustainable construction materials keeps increasing. However, as the most common material, concrete accounts for about 8% of global total carbon emissions and faces the scarcity of raw materials like high-quality sand and limestone (Ueda et al., 2020). Therefore, new eco-friendly construction materials with abundant raw materials that can partly substitute concrete are needed. One way is to use geopolymers. Ranjbar (Ranjbar et al., 2020) obtained tough materials from fly ash under 350°C. However, to reduce greenhouse gas emission, 30 nations including the U.K., Canada, France, and Mexico have committed to phase out the use of coal and decommission coal power stations and blast furnaces (Trencher et al., 2019). Consequently, as by-products, the global yields of FA and GBFS are shrinking, which limits their industrial usage. Low-quality sand (defined as the sand that particle size smaller than 250 µm) such as desert sand is abundant and therefore can be an alternative. However, according to GB/T 14684-2011 standard, the average particle size of sand should be around 350 -500 µm and the content of the very fine sand (particle size smaller than 250 µm) should be controlled within 10 mass% because too much fine sand results in high water absorption, impermeability, and insufficient structural strength. As a result, the utilization of low-quality sand is limited for the current concrete even though it is abundant.

Space exploration is accelerating globally, and moon may be the first satellite candidate for possible development. Lunar sulfur concrete (Toutanji et al., 2012) is widely studied because of its high compressive strength and no usage of water. However, sulfur is lacked on the moon

(< 1% by mass) and easy to be sublimed, indicating low durability (Wilhelm & Curbach, 2014). Considering Si is the second abundant element on the moon, moon sand can offer an alternative solution. Nevertheless, the moon sand is low-quality sand and hence the application is limited. Therefore, one way to make full use of low-quality sand should be studied. Sakai (Sakai & Farahani, 2021) has transformed sand into construction materials via autoclaving method under 240°C. However, the compressive strength was low and the reaction temperature was relatively high, which increases challenges for industrial production. Considering the average day-time temperature on the moon is about 110°C, this study aims to improve the strength and reduce the reaction temperature to 110°C, at which a pressure cooker can produce this condition easily. Inspired by the formation of a geopolymer, a low-temperature (110°C) sol-gel technology can be used to synthesise tough materials from low-quality sand. Based on the generation mechanism of geopolymers, the dissolution and reorganisation of $[\text{SiO}_4]^{4-}$ and $[\text{AlO}_4]^{5-}$ (Duxson et al., 2007) can occur through a reversible reaction (Eq. (1)). During this process, new crystals can be formed, which can fill the gap between sand particles and enhance the strength. Owing to the better wettability of ethanol (Yan et al., 2020) and better stability of TEOS (Saito et al., 1995), the reaction between sand and ethanol occurs more readily than that between sand and water. TEOS, as a good consolidate, can further improve the strength. Thus, a relatively low reaction temperature (110°C) is possible in the ethanol environment for both terrestrial and extraterrestrial construction.



To the best of our knowledge, the synthesis of tough construction material from low-quality sand in the ethanol environment has been reported only by the authors' research group. The present work is aimed at (1) transforming low-quality sand into a tough building material under 110°C and revealing the hardening mechanism; (2) studying the effect of KOH content and ethanol concentration on the compressive strength of the solidified specimen and improving the strength; (3) recycling the waste solution and calculating the CO₂ emission in the construction phase. The experimental results are expected to provide practical information on the hydrothermal synthesis of tough construction materials from useless but abundant low-quality sand with waste solution recycled. The new materials can alleviate the problem of insufficient concrete raw materials and provide an idea for extra-terrestrial construction simultaneously.

2 Experimental sections

2.1 Materials

Silica sand was purchased from ST Craft Ltd. (Hyogo, Japan), ethanol (C₂H₅OH, 99.5%, guaranteed reagent grade) from Wako Pure Chemical Industries Ltd., and potassium hydroxide (KOH, reagent grade) from Merck Co., Ltd. The chemical composition of the sand was measured using X-ray fluorescence spectroscopy (XRF, ZSX Primus IV, Rigaku Corporation, Tokyo, Japan) and the results are shown in Table 1. The main components of the sand are SiO₂ and Al₂O₃, along with some K₂O. The X-ray diffractometry (XRD, Multiflex Rigaku, Tokyo, Japan) result (Fig. 1) shows that the main phases of the sand are quartz (Q, SiO₂), kaolinite (K, Al₂Si₂O₅(OH)₄), and Muscovite (M, KAl_{2.2}(Si₃Al)_{0.975}O₁₀(OH)_{1.72}O_{0.28}). From the particle size distribution (SYNC-ST01, MicrotracBEL Corp., Tokyo, Japan) of the sand (Fig. 2), it can be

found that 98.5% of the sand has a particle size smaller than 250 μm , indicating that the raw sand selected is low-quality sand.

Table 1 Chemical composition of raw sand [mass%].

Composition	SiO ₂	Al ₂ O ₃	K ₂ O	TiO ₂	Fe ₂ O ₃	Na ₂ O	CaO	MgO	ZrO ₂	LOI
Content	84.70	8.47	4.71	0.70	0.68	0.26	0.15	0.12	0.08	0.13

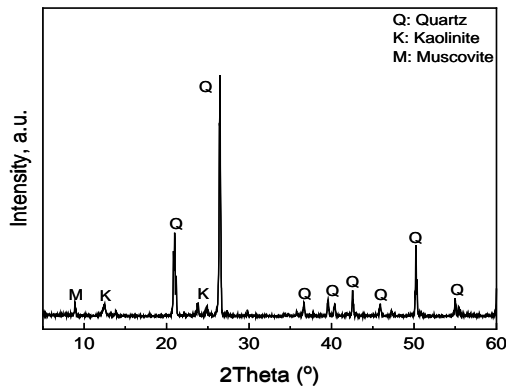


Fig. 1 X-ray diffraction pattern of raw sand.

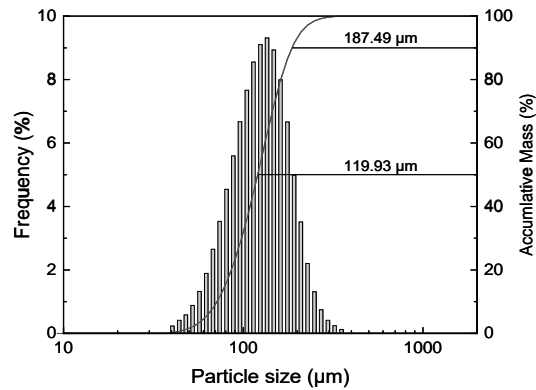


Fig. 2 Particle size distribution of raw sand.

2.2 Preparation of specimens

The sand was mixed with 0 mass% - 40 mass% KOH (mass% means the weight percent of KOH against sand), which was then placed in a cylindrical container made from stainless foil and the autoclave. Different concentrations of ethanol (0–99.5% V/V, 15 ml) was added (Fig. 3a). Autoclaves were heated under saturated ethanol vapour pressure at 110°C for 7 days. Wet powder could be obtained with waste solution. Wet powder was hot-pressed under 105°C and 2.5 MPa for 1 min and then dried at 105°C for another 7 days, which were finally sintered at 500°C for 3 h (Fig. 3b). Three samples were prepared for each condition.

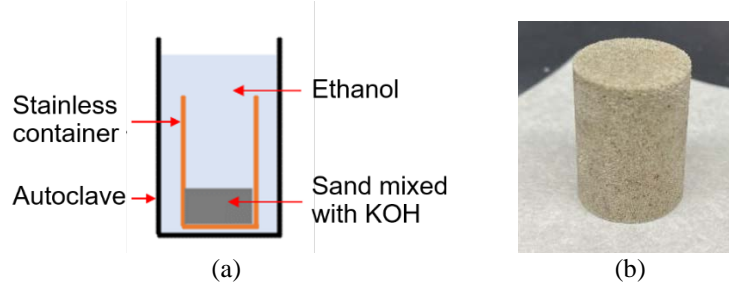


Fig. 3 (a) Schematic of mixed raw materials (b) Prepared sample.

2.3 Characterisation

The porosity of the specimens ($\Phi 20 \text{ mm} \times 30 \text{ mm}$) was measured using the Archimedes principle based on the GB/T 8489-2006 standard. The compressive strength was measured at a loading rate of 0.5 kN/min using a universal testing machine (UH-1000kNC, Shimadzu, Tokyo, Japan). The crushed specimens were then investigated by XRD at 40 kV and 30 mA using Cu K α radiation ($\lambda = 1.54 \text{ \AA}$, 2θ : 5–60°, 0.02°/s) and FT-IR (FT/IR 4100, JASCO, Tokyo, Japan) via the KBr pellet technique.

2.4 Waste solution recycling

Waste solution was evaporated through the rotary evaporator (EYELA N-1300, Tokyo) with a rotation speed of 30 rpm and pressure of 4 kPa in a water bath held at 30°C. The recycle rate (r) is calculated by $r = m_1/m_0$, where m_0 , m_1 means the raw ethanol and the weight of recycled ethanol. The average recycle rate is about 65.75%

2.5 Carbon emission calculation using SimaPro

The principles of lifecycle cost analysis were taken as the guiding principle, and the Building for Environmental and Economic Sustainability (BEES) method in the SimaPro software (TCO2 Co., Ltd., Tokyo, Japan) was selected to conduct a quantitative study of the research case. Environmental V3 database in the inventory database was selected in this study.

The system boundary and methodology framework for this study are shown in Figs. 4 and 5. First, the functional unit was defined as an effective building area of 1 m² (Li et al., 2019) and the lifetime of sand-based construction materials was assumed 50 years. Second, it was assumed that the material transportation distance was 20 km. Further, the electricity for autoclaving, hot-press, drying and sintering was estimated as 75.75 kWh/m², 0.168 kWh/m², 89.54 kWh/m², and 3.82 kWh/m², respectively, based on prior studies (Quiros et al., 2015; Worrell et al., 2001). This study focused on the calculation of CO₂ emission in the construction phase whereas the emissions in the using and disposal phases are not discussed in this paper. The specimen with 20% KOH and 90% ethanol concentration was selected to calculate the CO₂ emission.

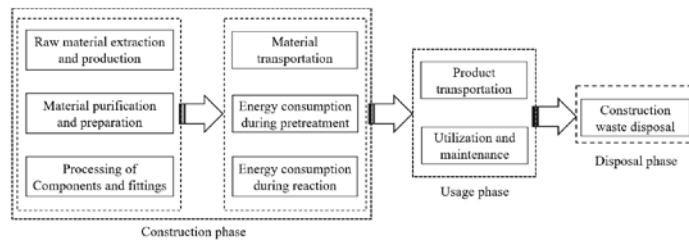


Fig. 4 System boundary of the sand-based construction material.

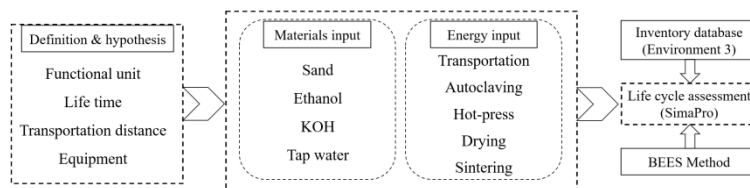


Fig. 5 Methodology framework.

3. Results and discussion

3.1 Compressive strength and porosity

3.1.1 Effect of EtOH concentrations

Ethanol, as one of the main reactants, plays the key role to control the degree of the reaction. The compressive strength and porosity development of the specimens with different EtOH

concentrations are shown in Fig. 6. The compressive strength is about 7.85 MPa at EtOH concentration of 99.5%, which is enhanced to 38.55 MPa when EtOH concentrations decreases to 90%. Afterwards, the compressive strength decreases gradually with further reducing EtOH concentrations. The porosity first decreases with reducing EtOH concentration, reaching the minimum (17.93%) at 90%. Then, it increases to 27.29% at 60% EtOH concentration. It appears that the decrease in porosity may be the reason for the increase in strength. XRD analyse was conducted to study the reason for the decrease in porosity.

Fig. 7 shows the phase evolution of the above specimens. Compared with raw sand (Fig. 1), the peak intensity of quartz, kaolinite and muscovite decreases with the increase of EtOH concentration. It indicates that higher degree of the forward reaction between raw sand and EtOH under higher EtOH concentration. Concurrently, new peaks that belong to zeolite form when EtOH concentration increases to 90%. The peak of sanidine can be observed after the reaction. However, its peak intensity tends to decrease with reducing EtOH concentration. It might be because high EtOH concentration limits the reverse reaction in Eq. (1) and the reorganization of Si-O-Si bonds. The formation of both zeolite and sanidine could fill the gap between particles and therefore enhance the strength. Combined with the trend of compressive strength (Fig. 6), 90% EtOH seems to be the most appropriate concentration with both the formation of zeolite and relatively high content of formed sanidine.

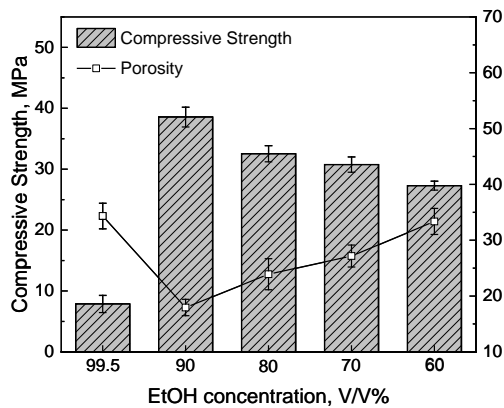


Fig.6 Compressive strength and porosity developments of specimens with different ethanol concentrations

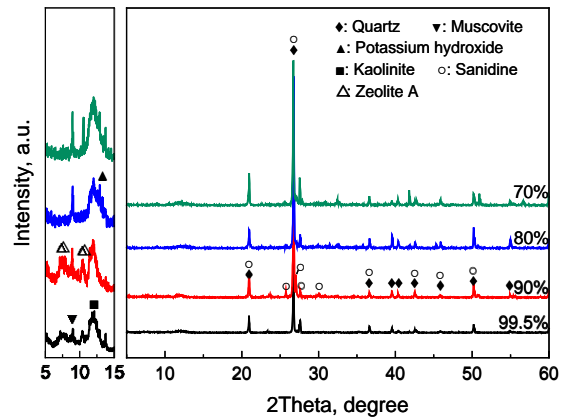


Fig.7 XRD patterns of specimens with different ethanol concentrations.

3.1.2 Effect of KOH contents

KOH may function as both the catalyst (Fukaya et al., 2017) and the reactant (Duxson et al., 2007), so KOH has key effect on the compressive strength. Fig. 8 shows the compressive strength and porosity development of the specimens mixed with different quantities of KOH. Without KOH content, hardened body cannot be made. After adding KOH, the compressive strength first increases with the increasing content of KOH and reaches the maximum (38.55 MPa) at 20 mass% KOH content. Afterwards, the compressive strength decreases with further addition of KOH. In contrast, the porosity first decreases with increasing KOH content until 20 mass% and then gradually increases with further addition of KOH. To study the reason of compressive strength change trend, FTIR analysis was conducted.

Fig. 8 shows the FTIR spectra of the above specimens with different KOH contents. The broad peak at 3440 and 3211 cm^{-1} belongs to the O–H stretching vibrations generated by water and Si–OH. The band at 1639 cm^{-1} is attributed to the H–O–H bending vibrations of the interlayer water of silicate. The sample with 0 mass% KOH exhibited peaks at 1084, 775, 692, 529, and 466 cm^{-1} , which belong to the Si–O–Si or Si–O–Al stretching of quartz and kaolinite (Qiu et al., 2018). The peak intensity of them tends to be weakened with increasing KOH content. According to XRD results (Fig. 7), they tend to transform into sanidine and zeolite. In addition, new bonds appear at 2921, 2852, 1465, and 1384 cm^{-1} and 880 cm^{-1} , which should belong to the C–H and Si–O–C stretching of TEOS respectively (Rubio et al., 1998; Stefanescu et al., 2007). The peak intensity tends to be enhanced with increasing KOH content. A previous study (Barberena-Fernandez et al., 2015) showed TEOS can function as consolidate and therefore is beneficial for strength enhancement. New peaks at 2240, 2140, 2010 cm^{-1} can be seen when the KOH content is above 30 mass%, which correspond to triple bonds and cumulative double bonds. The formation of these peaks might be because of the side reaction of the ethanol under high alkaline environment, which has negative influence on the compressive strength. Therefore, combined with the strength development (Fig. 8), the formation of TOES, sanidine and zeolite may be the main reason for the increase in strength from 0 mass% to 20 mass% KOH content. However, further addition of KOH leads to the side reactions of EtOH. As a result, triple bonds and cumulative bonds tend to form and cause the decrease of the strength.

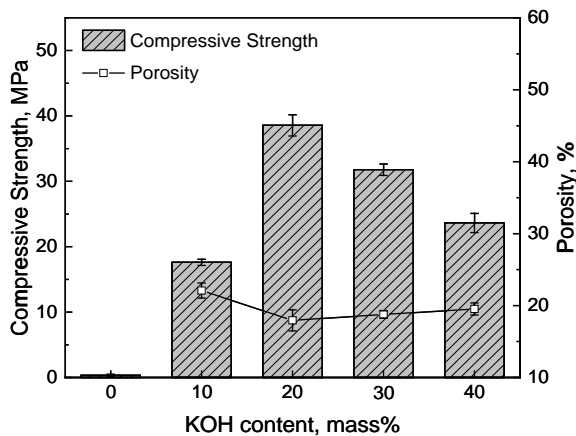


Fig.8 Compressive strength and porosity developments of specimens with different KOH contents.

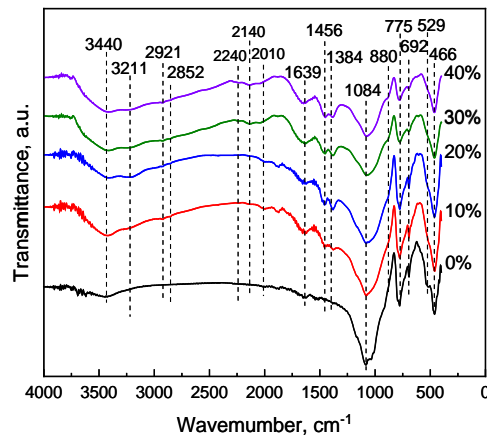


Fig.9 FT-IR spectra of samples containing different KOH contents

3.2 Carbon emission calculation

The quantities of raw materials per unit area of the sand-based construction material and the calculation results are shown in Table 2. The total carbon emission of the sand-based construction material is 325 kg CO_2 eq. Ethanol and construction electricity account for 194 kg CO_2 eq (60%) and 88 kg CO_2 eq (27%) respectively, which constitute nearly 90% of the total emission. The total carbon emissions can be reduced to 197 kg CO_2 eq after recycling waste solution, which is only 35.82% of that produced by normal concrete (550 kg CO_2 eq) (Guggemos & Horvath, 2005). Furthermore, considering the autoclaving temperature (110°C),

and hot-press and drying temperature (105°C) is low, heat waste could be used. As a result, the total carbon emissions could be further reduced.

Table 2 Main constituents of sand-based construction material per functional unit area [m⁻²] and carbon emissions of sand-based construction material in the construction phase.

Input	Unit	Value	Carbon emissions /kg CO ₂ eq	Percentage /%
Sand	kg	76.51	3.30	1.02
Ethanol	kg	217.45	194.23	59.79
KOH	kg	15.30	37.98	11.69
Tap water	kg	2.37	0.00050	0.00
Transpiration	kgkm	6500	1.07	0.33
Electricity	kWh	169.13	88.27	27.17
Summary			324.86	100

4. Conclusions

The sol-gel method was used to transform low-quality sand into a tough and green construction material directly under 110°C. The results are summarised as follows:

(1) A tough (compressive strength 38 MPa) construction material can be synthesised from low-quality sand under 110°C. The formation of sanidine, zeolite, and TEOS were found to enhance the strength. The formed sanidine, zeolite can fill the gap between the particles whereas TEOS is a good consolidate that can function as a glue.

(2) The compressive strength is greatly influenced by the KOH content and ethanol concentration. The appropriate KOH content and ethanol concentration can improve the compressive strength. The specimen using 20 mass% KOH and 90% EtOH concentration has the highest strength.

(3) The tough construction material obtained from low-quality sand under low temperature is eco-friendly. The carbon emissions produced by the sand-based material in the construction phase can be as low as 197 kg CO₂ eq, which can be further reduced if waste heat can be used.

Acknowledgements

This work was supported by JST FOREST Program (Grant Number JPMJFR205P, Japan). This work was supported by Nanotechnology Platform project by the Ministry of Education, Culture, Sports, Science and Technology of Japan. The grant number JPMXP09A22UT0239.

Compliance with Ethical Standard

References

- Barberena-Fernandez, A. M., Carmona-Quiroga, P. M., & Blanco-Varela, M. T. (2015, Jan). Interaction of TEOS with cementitious materials: Chemical and physical effects. *Cement & Concrete Composites*, 55, 145-152. <https://doi.org/10.1016/j.cemconcomp.2014.09.010>
- Duxson, P., Fernández-Jiménez, A., Provis, J. L., Lukey, G. C., Palomo, A., & van Deventer, J. S. J. (2007, 2007/05/01). Geopolymer technology: the current state of the art. *Journal of Materials Science*, 42(9), 2917-2933. <https://doi.org/10.1007/s10853-006-0637-z>

- Fukaya, N., Choi, S. J., Horikoshi, T., Kataoka, S., Endo, A., Kumai, H., Hasegawa, M., Sato, K., & Choi, J. C. (2017, Mar). Direct synthesis of tetraalkoxysilanes from silica and alcohols. *New Journal of Chemistry*, 41(6), 2224-2226. <https://doi.org/10.1039/c6nj03897b>
- Guggemos, A. A., & Horvath, A. (2005, Jun). Comparison of Environmental Effects of Steel- and Concrete-Framed Buildings. *Journal of Infrastructure Systems*, 11(2), 93-101. [https://doi.org/10.1061/\(asce\)1076-0342\(2005\)11:2\(93\)](https://doi.org/10.1061/(asce)1076-0342(2005)11:2(93))
- Li, H., Deng, Q., Zhang, J., Xia, B., & Skitmore, M. (2019, Feb 10). Assessing the life cycle CO₂ emissions of reinforced concrete structures: Four cases from China. *Journal of Cleaner Production*, 210, 1496-1506. <https://doi.org/10.1016/j.jclepro.2018.11.102>
- Qiu, P., Jing, Z., Liu, Z., Yujie, Q. I., & Miao, J. (2018). Wet Preparation and Hardening Mechanism of Calcium Carbonate Based Building Materials. *Journal of Building Materials*, 2, 241-246, 313. <https://doi.org/10.3969/j.issn.1007-9629.2018.02.011>
- Quiros, R., Gabarrell, X., Villalba, G., Barrera, R., Garcia, A., Torrente, J., & Font, X. (2015, Nov 16). The application of LCA to alternative methods for treating the organic fiber produced from autoclaving unsorted municipal solid waste: case study of Catalonia. *Journal of Cleaner Production*, 107, 516-528. <https://doi.org/10.1016/j.jclepro.2014.04.018>
- Ranjbar, N., Kashefi, A., Ye, G., & Mehrali, M. (2020, Jan 20). Effects of heat and pressure on hot-pressed geopolymer. *Construction and Building Materials*, 231, Article 117106. <https://doi.org/10.1016/j.conbuildmat.2019.117106>
- Rubio, F., Rubio, J., & Oteo, J. L. (1998). A FT-IR study of the hydrolysis of tetraethylorthosilicate (TEOS). *Spectroscopy Letters*, 31(1), 199-219. <https://doi.org/10.1080/00387019808006772>
- Saito, Y., Isobe, T., & Senna, M. (1995, Nov 15). INCIPIENT CHEMICAL-REACTION ON THE SCRATCHED SILICON(111) SURFACE WITH ETHOXY AND HYDROXY-GROUPS. *Journal of Solid State Chemistry*, 120(1), 96-100. <https://doi.org/10.1006/jssc.1995.1382>
- Sakai, Y., & Farahani, A. (2021). Production of hardened body by direct bonding between sand particles. *SEISAN KENKYU*, 73(3), 185-188. <https://doi.org/10.11188/seisankenkyu.73.185>
- Stefanescu, M., Stoia, M., Stefanescu, O., Popa, A., Simon, M., & Ionescu, C. (2007, Apr). The interaction between TEOS and some polyols - Thermal analysis and FTIR. *Journal of Thermal Analysis and Calorimetry*, 88(1), 19-26. <https://doi.org/10.1007/s10973-006-8002-7>
- Toutanji, H. A., Evans, S., & Grugel, R. N. (2012, Apr). Performance of lunar sulfur concrete in lunar environments. *Construction and Building Materials*, 29, 444-448. <https://doi.org/10.1016/j.conbuildmat.2011.10.041>
- Trencher, G., Healy, N., Hasegawa, K., & Asuka, J. (2019, Sep). Discursive resistance to phasing out coal-fired electricity: Narratives in Japan's coal regime. *Energy Policy*, 132, 782-796. <https://doi.org/10.1016/j.enpol.2019.06.020>
- Ueda, H., Sakai, Y., Kinomura, K., Watanabe, K., Ishida, T., & Kishi, T. (2020, Jan). Durability Design Method Considering Reinforcement Corrosion due to Water Penetration. *Journal of Advanced Concrete Technology*, 18(1), 27-38. <https://doi.org/10.3151/jact.18.27>
- Wilhelm, S., & Curbach, M. (2014, Sep). Review of possible mineral materials and production techniques for a building material on the moon. *Structural Concrete*, 15(3), 419-428. <https://doi.org/10.1002/suco.201300088>
- Worrell, E., Price, L., Martin, N., Hendriks, C., & Meida, L. O. (2001). Carbon dioxide emissions from the global cement industry. *Annual Review of Energy and the Environment*, 26, 303-329. <https://doi.org/10.1146/annurev.energy.26.1.303>
- Yan, Y., Wang, Z., Wang, D., Cao, J., Ma, W., Wei, K., & Yun, L. (2020, Jul). Recovery of Silicon via Using KOH-Ethanol Solution by Separating Different Layers of End-of-Life PV Modules. *JOM*, 72(7), 2624-2632. <https://doi.org/10.1007/s11837-020-04193-6>